Research Article



# Model predictive control for voltage restoration in microgrids using temporal logic Accepted on 14th April 2020 specifications

eISSN 2516-8401 Received on 1st December 2019 Revised 28th March 2020 doi: 10.1049/iet-esi.2019.0135 www.ietdl.org

Fatima Z. Taousser¹, Mohammed M. Olama² ⋈, Seddik M. Djouadi¹, Kevin Tomsovic¹, Yichen Zhang³, Yaosuo Xue⁴

<sup>1</sup>Department of Electrical Engineering and Computer Science, University of Tennessee, Knoxville, TN 37996, USA

Abstract: Power system operation will encounter numerous voltage variabilities as the proliferation of renewable energy continues. Real-time monitoring and communication technologies can potentially improve voltage stability by enabling the rapid detection of voltage deviations and the implementation of corrective actions. These corrective actions will only be effective in restoring stability if they are chosen in a timely and scalable manner. This study considers the problem of power systems' load voltage control in order to simultaneously address both magnitude and time voltage specifications. In order to comply with grid codes and avoid unnecessary relay protection actions, a model predictive control-based control strategy employing temporal logic specifications (TLSs) is proposed. The TLSs strategy is introduced as a formalism to control the voltage variation at a critical load bus against operational bounds over time. The control objective is to schedule optimal control input signals from the available supportive energy storage systems, which provide reactive power injections, leading to satisfying the specified finitetime restoration described by the TLSs with minimal control efforts. The simulation results display that the TLSs strategy for power systems' voltage control synthesis is extremely significant.

#### 1 Introduction

Voltage stability refers to the ability of a power system to maintain acceptable voltage under normal conditions and after disturbances. Voltage instability occurs when a power system is unable to meet the reactive power demand and is usually corrected by injecting reactive power at some critical buses using energy storage devices [1]. Since the coordinating actions in power systems taken over large networks are complex, the corrective actions are traditionally performed as local controls to limit complexity [1]. With the incorporation of renewable energy in the ancillary services, energy storage systems (ESSs), such as flywheels, capacitors, and batteries, serve as buffers for the power system to restore critical bus voltages to the allowable ranges [2].

In recent years, power systems have increasingly been utilising diversified power resources to provide more reliable and efficient ancillary services [3, 4]. Note that ESSs perform better than traditional generators and operating reserves with their quicker responsive capabilities [5]. The question for load voltage control is how to keep the system voltage within a permissible level through the local control of each bus [6]; this is usually represented as a set of range (magnitude) specifications and constraints. Many works have been devoted to such specifications of power systems control design with only range constraints [7, 8]. However, realistic power system operations are based on range-valued mappings and on temporal properties. A typical example is relay settings, since an underfrequency relay will be triggered if the frequency stays within the triggering zone for a few cycles. Moreover, sophisticated grid codes that include voltage and frequency temporal properties have been proposed for distributed energy resources (DERs) [8] according to the many recent standards, such as the IEEE 1547 standard. A natural outcome of these characteristics is the development of a tool that can specify both time and range (magnitude) requirements in the control design. Furthermore, different DERs have different response times, and thus, their voltage supports have different time restoration properties. These realistic operational requirements have motivated us to develop

grid support controllers based on temporal logic specifications (TLSs) that can be integrated into DERs to satisfy more sophisticated time and range specifications. TLSs allow addressing both range and time specifications simultaneously.

Secondary voltage control of critical buses is important to regulate equipment operation at nominal values, especially under intermittent renewable generations and constantly changing load demands [6]. Note that, in a well-maintained power system, the voltage magnitude typically varies within 5% of the nominal value. Many works have been devoted to this area [4, 6–14], where most specifications of system control design are only focused on range constraints, in which the voltage level must be kept within specified limits. In order to avoid unnecessary relay actions and comply with grid codes and different response times of DERs, constraints of dwell times on specified ranges need consideration. Notice that failure to consider such critical time constraints may lead to cascading outages [4]. Thus, finite-time restoration and dwell time constraints are pressing and require a novel control paradigm and algorithm. Inspired by that, the TLSs strategy is introduced in this paper as a formalism to control voltage variations at a critical load bus against operational bounds over

In this paper, we investigate the control synthesis from TLSs, based on a model predictive control (MPC) framework, to yield an optimal control policy. The main advantage of MPC is that it optimises the current operation while taking into account the predicted behaviour of the state variables over a future time horizon, and the optimal controller is designed based on the system model and the predicted behaviour. The controller uses the knowledge of the future behaviour and chooses the best actuation that will meet the predefined optimisation. Advances in MPC optimisation algorithms have enabled this control strategy for new classes of systems such as very large-scale systems and systems with fast dynamics. Another advantage of MPC is its ability to approximate and solve most optimal control problems numerically with much lower computational effort than the classical approaches like dynamic programming. MPC can handle much bigger

<sup>&</sup>lt;sup>2</sup>Computational Sciences and Engineering Division, Oak Ridge National Laboratory, Oak Ridge, TN 37831, USA

<sup>&</sup>lt;sup>3</sup>Energy Systems Division, Argonne National Laboratory, Lemont, IL 60439, USA

<sup>&</sup>lt;sup>4</sup>Electrical and Electronics Systems Research Division, Oak Ridge National Laboratory, Oak Ridge, TN 37831, USA ⋈ E-mail: olamahussemm@ornl.gov

problems and also has a unique ability to handle system limitations simply by adding them as constraints in the optimisation formulation. In MPC, a cost function is minimised over a short-time horizon using the predicted information, and only the first step control strategy is implemented. Such a process repeats at every time step yielding new control strategies. This ability and the greater coordination in multivariate systems frequently lead to greater profits and improved performance.

The objective in this work is that during a disturbance, the voltage is required to be restored back above a certain value within a required time utilising the support of the ESSs. The controller locally measures the voltage, estimates the size of disturbance, and computes the reactive power input for the ESS to be injected to the bus, such that the voltage variation satisfies the TLSs. The optimal control input is computed iteratively based on a finite horizon optimisation over the system in order to minimise the reactive power input from the ESS (control effort) using the MPC technique. At any given time t, the current system state is observed, and an optimal control strategy is computed for some finite time horizon in the future, [t, t + H]. An online calculation is performed to explore system trajectories originating from the current state, and an optimal control is computed up to time t + H. The MPC is designed by taking into consideration the limitations of the system, which are the ESS capacity, the maximum charge power available, and the permissible voltage deviation. Note that the ESS, which can meet voltage restoration using MPC design, has a precise timerelated performance measure, which can create economic benefit and affect the lifetime of the ESS.

When a fault or disturbance occurs in the power grid, the control objective in this work is to schedule optimal control input signals to the supportive ESSs, which provide reactive power injections, such that the voltages at the critical buses are restored to permissible levels within a specified time duration (satisfying the specified finite-time restoration described by the TLS) with minimal control efforts. To illustrate the effectiveness of this approach, the results are compared to that of control without TLSs, where it is observed that the voltage may take more time to restore to the desired level (violate the finite-time voltage restoration).

The pioneering works in [15, 16] introduce the TLSs for controller synthesis of ESSs, where a finite-time restoration is satisfied, by employing the control auto-bisimulation function and feedback linearisation control methods. Xu et al. [16] derive a provable probabilistic guarantee in the stochastic environment of a wind power generation. In [17, 18], a numerical optimal control (NOC)-based control synthesis approach is proposed to schedule a controller for frequency and voltage support, respectively, to satisfy the TLSs. In this paper, a mixed-integer programming (MIP) approach based on [17] is adopted. The MIP-based methods attain sub-optimal solutions at the cost of higher computational demand. From the problem-solving perspective, we introduce this framework to a new class of problems, namely, the voltage restoration in microgrids that is highly time-sensitive and includes control logics. The temporal logic constraints are imposed on the algebraic variables. Most linearisation and model reduction techniques will eliminate the algebraic variables, and thus are not applicable. On the other hand, the non-linear MIP is computationally expensive, therefore, linearised output models are derived to address this issue.

Temporal logic can be introduced to provide time-related specifications, such as after a fault, the voltage at a critical bus should be restored to a specified magnitude within a specified time duration. The TLSs approach was originally developed in order to specify and monitor the expected behaviour of physical systems, including temporal constraints between events. It allows richer descriptions of specifications including set, logic, and time-related properties [19–21]. There is a lot of literature on the control of ESSs in power systems for voltage support, while incorporating temporal logic constraints into the control synthesis problem is novel

## 2 Preliminaries on TLSs

The TLS approach is a formal math's language for describing time propositions. TLS provides a particularly useful set of operators to construct time properties without specifying sets. It uses formal logical manipulations to show that a property is satisfied for a given system model. The TLS language can be expressed with two kinds of operators: logical connectives (conjunction  $(\land)$ , disjunction ( $\vee$ ), negation ( $\neg$ ), application ( $\rightarrow$ ), and equivalence  $(\leftrightarrow)$ ), and temporal modal operators (eventually  $(\diamondsuit)$ , always  $(\Box)$ , and until ( $\mathcal{U}$ )). An atomic proposition  $\phi$  describes a feature of the system variables and maps on the Boolean domain  $\mathbb{B} = \{True, False\}$ . The validity of a formula  $\phi$  with respect to signal x is defined as  $x \models \phi$ . Informally,  $\Diamond \phi := \text{true } \mathcal{U} \phi$  (i.e.  $\phi$  will become true at some point in the future),  $\Box \phi := \neg \Diamond \neg \phi$  (i.e.  $\phi$  is always true (never eventually  $(\neg \phi)$ )). Additionally, we define  $x \models \Diamond_{[t_1,t_2]} \phi$  if the property defined by  $\phi$  holds at some time step between  $t_1$  and  $t_2$ , and we define  $x \models \Box_{[t_1,t_2]} \phi$  if  $\phi$  holds at every time step between  $t_1$  and  $t_2$ . An example of a TLS is  $\phi = \Box \neg (x_1 > 10) \land \Box_{[1,3]}(x_2 > 5)$ , which reads that 'x<sub>1</sub> is always less than 10, and  $x_2$  is always greater than 5 at each time step between the time interval from 1 to 3 s'

#### 2.1 System dynamics

We consider the continuous-time state-space system of the form

$$\dot{x} = f(x, u, w) 
y = g(x, u, w)$$
(1)

where  $\mathbf{x} \in \mathcal{X} \subseteq \mathbb{R}^n$  is the system state vector,  $u \in U \subseteq \mathbb{R}^m$  is the control input,  $w \in \mathcal{W} \subseteq \mathbb{R}^l$  is the perturbation, and  $y \in \mathcal{Y} \subseteq \mathbb{R}^r$  is the system output. Given a sampling time  $\Delta t = t_{k+1} - t_k$ , where  $k \in \mathbb{I} = \{0, 1, ...\}$  is the time index set, assume that the system (1) admits a discrete-time representation of the form

$$x(t_{k+1}) = f(x(t_k), u(t_k), w(t_k))$$
  

$$y(t_k) = g(x(t_k), u(t_k), w(t_k)).$$
(2)

Given an integer N > 0,  $x_0 \in \mathcal{X}$ , and the sequences  $\mathbf{x}^N = x_0 x_1, \dots, x_{N-1} \in \mathcal{X}^N$ ,  $\mathbf{u}^N = u_0 u_1, \dots, u_{N-1} \in U^N$  and  $\mathbf{w}^N = w_0 w_1, \dots, w_{N-1} \in \mathcal{W}^N$ , where  $x_k = x(t_k)$ ,  $u_k = u(t_k)$  and  $w_k = w(t_k)$ , for  $k \in \mathbb{L}$ . The resulting horizon-N vuv1 of (2) is a sequence

$$\varphi(x_0, \mathbf{u}^N, \mathbf{w}^N) = (x_0 u_0 w_0)(x_1 u_1 w_1), \dots, (x_N u_N w_N)$$

satisfying the equations in (2), which is unique (see [22]).

#### 2.2 Control synthesis

In this section, we formally state the TLSs control synthesis and its MPC formulation. Given a TLS proposition  $\phi$ , and a cost function of the form  $J(x_0, \boldsymbol{u}, \boldsymbol{w}, \phi) \in \mathbb{R}$ . We are interested in this paper by the closed-loop synthesis which can be stated as follows: Given a horizon 0 < L < N, for all  $0 \le k \le N - L$ , compute the first element of the sequence  $\boldsymbol{u}_k^L = u_k^L u_{k+1}^L$ , ...,  $u_{k+L-1}^L$  satisfying

$$\mathbf{u}_{k}^{L} = \underset{u_{k}^{L} \in U^{L}}{\operatorname{arg min}} J(x_{0}, \mathbf{u}_{k}^{L}, \mathbf{w}^{N}),$$

$$\mathbf{s} \ \mathbf{t} \cdot \boldsymbol{\omega}(x_{0}, \mathbf{u}_{k}^{L}, \mathbf{w}^{N}) \models \boldsymbol{\phi}.$$
(3)

The closed-loop formulation corresponds to an MPC scheme. Note that a TLS  $\phi$  is bounded time, and the bound is the maximum over the summation of all nested upper bounds on the temporal operators. For example, if  $\varphi = \diamondsuit_{[0,15]} \square_{[0,7]} \phi$ , then, we should require  $N \ge 15 + 7 = 22$  in order to determine whether the formula  $\phi$  is feasible. This provides a conservative maximum trajectory reference length required to decide the feasibility of  $\phi$ .

## 3 Voltage control with TLSs

#### 3.1 Problem statement and system modelling

We consider the distribution system model shown in Fig. 1. Notice that diesel generators are combustion engine driven synchronous generators (SGs). So, a scaled-down SG is employed to describe the behaviour. ESSs are widely deployed in distribution systems and microgrids to compensate for fluctuations of renewable sources. Therefore, it is reasonable and sufficient to consider only the dispatchability of ESSs. Isolated microgrids are generally formed by disconnecting the distribution systems from the main grid. Such distribution systems (or isolated microgrids) are radial with backup diesel generators at the upstream grid and ESSs at the downstream grid. Based on this feature, any large-scale distribution system can be represented by the lumped grid shown in Fig. 1. Although the model is simplified, it does represent and describe the key behaviours of a typical diesel generator fed isolated microgrid. Note that in industrial practices, diesel generators are the major sources to power isolated microgrids as shown in [23, 24]. The system considered here represents a distribution bus fed through a transmission system equivalent. To increase transfer limits, the distribution system has been compensated by an ESS at the critical load bus. The perturbation is considered as a net load change at the critical bus (bus 2). Such a disturbance may represent a sudden change in renewable generation at the load side due to either the intermittency of renewable generation at the load side (due to the stochastic nature of renewable generation) or a sudden change in demand (due to big loads switch on/off at the same time).

The objective is to optimally control the reactive power input injected from the ESS, such that when a disturbance occurs, the voltage at the critical bus is restored to a permissible level within a specified time duration. The TLSs strategy is introduced to adopt this additional time constraint in order to avoid any unnecessary protective relay actions. To illustrate the effectiveness of this approach, the MPC is also designed for the system without TLSs as a base case, and the results are compared.

A one-axis flux-decay model dynamic circuit for the SG, as shown in Fig. 2, is considered. The overall system dynamic and algebraic equations, in addition to the load and transmission line characteristics, are presented next.

3.1.1 Generator model: The dynamic circuit for the flux-decay model of the SG in Fig. 2 is considered. The full state differential-algebraic equations are given by

$$\begin{split} \dot{\delta} &= \omega - \omega_{\rm s} \\ \dot{\omega} &= \frac{\omega_{\rm s}}{2H} [P_{\rm m} - (E'_q I_q + (X_q - X'_d) I_d I_q + D(\omega - \omega_{\rm s}))] \\ \dot{E}'_q &= \frac{-1}{T_{d_0}} [E'_q + (X_d - X'_d) I_d - E_{\rm fd}] \\ \dot{E}_{\rm fd} &= \frac{-1}{T_{\rm A}} [E_{\rm fd} - K(V_{\rm ref} - V_1)] \\ \dot{P}_{\rm m} &= \frac{-1}{T_{\tau}} [P_{\rm m} - P_{\rm v}] \\ \dot{P}_{\rm v} &= \frac{-1}{T_{\rm g}} \Big[ P_{\rm v} - \Big( P_{\rm ref} - \frac{1}{R} \Big( \frac{\omega}{\omega_{\rm s}} - 1 \Big) \Big) \Big] \\ R_{\rm e} I_d - (X_q + X_{\rm e}) I_q + V_2 {\rm sin} (\delta - \theta_2) = 0, \\ R_{\rm e} I_q + (X'_d + X_{\rm e}) I_d - E'_q + V_2 {\rm cos} (\delta - \theta_2) = 0, \end{split} \tag{5}$$

$$V_d = V_1 \sin(\delta - \theta_1) = X_q I_q,$$

$$V_q = V_1 \cos(\delta - \theta_1) = E'_q - X'_d I_d,$$
(6)

where  $\delta, \omega, \omega_{\rm s}, E'_q, E_{\rm fd}, P_{\rm m}, P_{\rm v}$  are the generator angle, frequency, synchronous frequency, q-axis transient voltage, field voltage, mechanical power, and steam valve position of the prime mover, respectively.  $\theta_1$  and  $\theta_2$  are the voltage phase angles at buses 1 and 2, respectively.  $I_d$ ,  $I_q$  and  $V_d$ ,  $V_q$  are the d-axis, q-axis currents and d-axis and q-axis voltages, respectively.  $X_d, X_q, X'_d$  are, respectively,

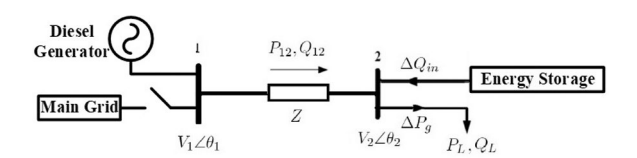


Fig. 1 Distribution system model

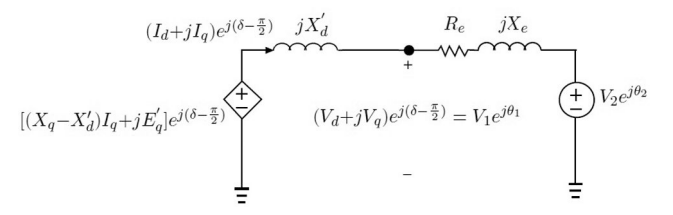


Fig. 2 Synchronous machine one-axis dynamic circuit

the *d*-axis reactance, *q*-axis reactance, and *d*-axis transient reactance.  $R_{\rm e}$  and  $X_{\rm e}$  are the external resistance and reactance, respectively.

The terminal voltage and the current are given by  $V_1 e^{j\theta_1} = (V_d + jV_a)e^{j(\delta - \frac{\pi}{2})}$  and  $I = (I_d + jI_a)e^{j(\delta - \frac{\pi}{2})}$ , respectively.

The linearisation of the algebraic equations in (5) around the steady-state operating point is given by

$$\Delta I_d = \alpha_1 \Delta V_2 + \alpha_2 [\Delta \delta - \Delta \theta_2] + \alpha_5 \Delta E'_q$$
  

$$\Delta I_q = \alpha_3 \Delta V_2 + \alpha_4 [\Delta \delta - \Delta \theta_2] + \alpha_6 \Delta E'_q$$
(7)

Similarly, by linearising the equations in (6), we get

$$\Delta I_d = \alpha_7 \Delta V_1 + \alpha_8 [\Delta \delta - \Delta \theta_1] + \alpha_9 \Delta E'_q$$
  
$$\Delta I_q = \alpha_{10} \Delta V_1 + \alpha_{11} [\Delta \delta - \Delta \theta_1]$$
 (8)

From (7) and (8), we derive the expressions of  $\Delta V_1$  and  $\Delta \theta_1$  as follows:

$$\Delta V_1 = \beta_1 \Delta V_2 + \beta_2 [\Delta \delta - \Delta \theta_2] + \beta_5 \Delta E'_q,$$
  

$$\Delta \theta_1 = \beta_3 \Delta V_2 + (\beta_4 + 1) \Delta \delta - \beta_4 \Delta \theta_2 + \beta_6 \Delta E'_q.$$
(9)

The constants  $\alpha_1 - \alpha_{11}$  and  $\beta_1 - \beta_6$  are determined in the Appendix. Suppose that the frequency is normalised as  $\omega_r = (\omega/\omega_s)$ . Linearising the dynamic equations in (4) by considering the expressions of  $\Delta I_d$  and  $\Delta I_q$  in (7), and  $\Delta V_1$  in (9), we get the following linearised system:

$$\begin{split} \Delta \dot{\delta} &= \omega_{\rm s} \Delta \omega_{\rm r} \\ \Delta \dot{\omega}_{\rm r} &= \frac{1}{2H} [\Delta P_{\rm m} - (K_1 \Delta \delta + K_2 \Delta E'_q + K_3 \Delta V_2) - D \Delta \omega_{\rm r}] \\ \Delta \dot{E}'_q &= \frac{-1}{T_{d_0}} [K_4 \Delta \delta + K_5 \Delta E'_q + K_6 \Delta V_2 - \Delta E_{\rm fd}] \\ \Delta \dot{E}_{\rm fd} &= \frac{-1}{T_A} [\Delta E_{\rm fd} - K[\Delta V_{\rm ref} \\ &- (\beta_1 \Delta V_2 + \beta_2 \Delta \delta + \beta_5 \Delta E'_q)]] \\ \Delta \dot{P}_{\rm m} &= \frac{-1}{T_\tau} [\Delta P_{\rm m} - \Delta P_{\rm v}] \\ \Delta \dot{P}_{\rm v} &= \frac{-1}{T_{\rm g}} [\Delta P_{\rm v} - \Delta P_{\rm ref} + \frac{1}{R} \Delta \omega_{\rm r}], \end{split}$$
(10)

where  $K_1 - K_9$  are also derived in the Appendix.

3.1.2 Load model: Bus 2 is considered as a load bus, where  $P_{\rm L}$  and  $Q_{\rm L}$  are the active and reactive load powers, respectively. A sudden net load change in the active power at bus 2 is considered as a disturbance and denoted by  $\Delta P_{\rm g}$ . The objective is to control the voltage deviation  $\Delta V_2$  by controlling the reactive power output

of the ESS injected to bus 2, denoted by  $\Delta Q_{\rm in}$ . Note that in this study, only reactive power support is considered.

3.1.3 Power flow network: Consider the line impedance  $Z = R_e + jX_e$ . The power flow across the transmission line from bus 2 to bus 1 is denoted by  $S_{21} = P_{21} + jQ_{21}$  and follows from Kirchhoff's laws as

$$S_{21} = V_2 e^{j\theta_2} I^* = V_2 e^{j\theta_2} \left( \frac{V_2 e^{j\theta_2} - V_1 e^{j\theta_1}}{Z} \right)^*, \tag{11}$$

which leads to the following non-linear algebraic equations:

$$P_{21} = G_{21}V_2^2 - V_1V_2(G_{21}\cos(\theta_2 - \theta_1) - B_{21}\sin(\theta_2 - \theta_1))$$

$$Q_{12} = B_{21}V_2^2 - V_1V_2(G_{21}\sin(\theta_2 - \theta_1) + B_{21}\cos(\theta_2 - \theta_1))$$
(12)

where

$$G_{21} + jB_{21} = \frac{1}{Z^*} = \frac{R_e}{R_e^2 + X_e^2} + j\frac{X_e}{R_e^2 + X_e^2}$$

The power balance at bus 2 is given by  $P_{21} + P_{L} + \Delta P_{g} = 0$ , and  $Q_{21} + Q_{L} - \Delta Q_{in} = 0$ . The linearised power flow equations are given by the following equation:

$$\Delta P_{21} = c_1 \Delta V_2 + c_2 \Delta V_1 + c_3 [\Delta \theta_2 - \Delta \theta_1] = -\Delta P_g$$
  

$$\Delta Q_{21} = c_4 \Delta V_2 + c_5 \Delta V_1 + c_6 [\Delta \theta_2 - \Delta \theta_1] = \Delta Q_{ip}$$
(13)

Substituting  $\Delta V_1$  and  $\Delta \theta_1$  by their values from (9) into (13), we get

$$\Delta V_2 = \gamma_1 \Delta \delta + \gamma_2 \Delta E_q' + \gamma_3 \Delta Q_{\rm in} + \gamma_4 \Delta P_{\rm g}. \tag{14}$$

The constants  $c_1 - c_6$  and  $\gamma_1 - \gamma_4$  are determined in the Appendix. Substituting  $\Delta V_2$  into (10) yields the final linearised system

$$\Delta \dot{\delta} = \omega_{s} \Delta \omega_{r}$$

$$\Delta \dot{\omega}_{r} = \frac{1}{2H} [\Delta P_{m} - (K'_{1} \Delta \delta + K'_{2} \Delta E'_{q} + K'_{3} \Delta Q_{in} + K'_{4} \Delta P_{g})$$

$$-D \Delta \omega_{r}]$$

$$\Delta \dot{E}_{q} = \frac{-1}{T_{d_{0}}} [K'_{5} \Delta \delta + K'_{6} \Delta E'_{q} + K'_{7} \Delta Q_{in} + K'_{8} \Delta P_{g} - \Delta E_{fd}]$$

$$\Delta \dot{E}_{fd} = \frac{-1}{T_{A}} [\Delta E_{fd} - K(\Delta V_{ref} - (K'_{9} \Delta \delta + K'_{10} \Delta E'_{q} + K'_{11} \Delta Q_{in} + K'_{12} \Delta P_{g}))]$$

$$\Delta \dot{P}_{m} = \frac{-1}{T_{r}} [\Delta P_{m} - \Delta P_{v}]$$

$$\Delta \dot{P}_{v} = \frac{-1}{T_{g}} [\Delta P_{v} - \Delta P_{ref} + \frac{1}{R} \Delta \omega_{r}]$$
(15)

Define the state vector as

$$X = \left[\Delta \delta \ \Delta \omega_{\rm r} \ \Delta E_{a} \ \Delta E_{\rm fd} \ \Delta P_{\rm m} \ \Delta P_{\rm v}\right]^{\rm T},$$

 $\Delta V_2 = \gamma_1 \Delta \delta + \gamma_2 \Delta E'_a + \gamma_3 \Delta Q_{in} + \gamma_4 \Delta P_g.$ 

and consider that  $\Delta V_{\rm ref} = \Delta P_{\rm ref} = 0$ . The simplified model in state-space form can be expressed as follows:

$$\dot{X} = AX + B_{u}\Delta Q_{in} + B_{w}\Delta P_{g}$$

$$\Delta V_{2} = CX + D_{u}\Delta Q_{in} + D_{w}\Delta P_{g}$$
(17)

where

$$A = \begin{bmatrix} 0 & \omega_{s} & 0 & 0 & 0 & 0 \\ \frac{-K'_{1}}{2H} & \frac{-D}{2H} & \frac{-K'_{2}}{2H} & 0 & \frac{1}{2H} & 0 \\ \frac{-K'_{5}}{T_{d_{0}}} & 0 & \frac{-K'_{6}}{T_{d_{0}}} & \frac{1}{T_{d_{0}}} & 0 & 0 \\ \frac{-KK'_{9}}{T_{A}} & 0 & \frac{-KK'_{10}}{T_{A}} & \frac{-1}{T_{A}} & 0 & 0 \\ 0 & 0 & 0 & 0 & \frac{-1}{T_{\tau}} & \frac{1}{T_{\tau}} \\ 0 & \frac{-1}{RT_{g}} & 0 & 0 & 0 & \frac{-1}{T_{g}} \end{bmatrix}$$

$$(18)$$

$$B_{\rm u} = \left[ 0 \, \frac{-K'_3}{2H} \, \frac{-K'_7}{T_{d_0}} \, \frac{-KK'_{11}}{T_{\rm A}} \, 0 \, 0 \right]^{\rm T} \tag{19}$$

$$B_{\rm w} = \left[ 0 \, \frac{-K'_4}{2H} \, \frac{-K'_8}{T_{d_0}} \, \frac{-KK'_{12}}{T_{\rm A}} \, 0 \, 0 \right]^{\rm T} \tag{20}$$

$$C = [\gamma_1 \ 0 \ \gamma_2 \ 0 \ 0 \ 0], \quad D_{\mathbf{u}} = \gamma_3, \quad D_{\mathbf{w}} = \gamma_4.$$
 (21)

See the Appendix for the expressions of constants  $K'_1 - K'_{12}$ .

### 3.2 Control diagram

In order to achieve the control policy with TLSs, the size of the disturbance will be estimated using the voltage measurement at bus 2. The estimated disturbance is sent to the online controller, where the derived model in (17) is embedded, as shown in the control diagram in Fig. 3. With both information on the disturbance and model, the controller in a receding horizon fashion computes a sequence of inputs at each time step, and only the first input value is used for the next time step, and the process iterates. The approach is based on encoding the system dynamics, the TLS constraints, and the cost function together in mixed-integer linear programming (MILP) [25], which is solved using an MPC framework by MILP solvers, yielding an optimal control policy. The encoding problem as a MILP formulation consists of system constraints, loop constraints, and TLS constraints.

#### 3.3 MPC formulation with TLS

Let the analytical model in (17) be expressed compactly as follows:

$$X(t_{k+1}) = A_d X(t_k) + B_{d1} u(t_k) + B_{d2} \hat{d}(t_k),$$

$$\Delta V_2(t_{k+1}) = C_d X(t_k) + D_{d1} u(t_k) + D_{d2} \hat{d}(t_k),$$
(22)

for  $k \in \mathbb{N}$ , where the control input  $u = \Delta Q_{\rm in}$  and the perturbation  $\hat{d} = \Delta P_{\rm g}$ . The objective is to design an optimal control u such that the following temporal constrain is satisfied:

$$\phi := \square[\neg(|\Delta V_2(t_k)| \le \Delta V) \Rightarrow \diamondsuit_{[0,t_a]}\square(|\Delta V_2(t_k)| \le \Delta V)]. \tag{23}$$

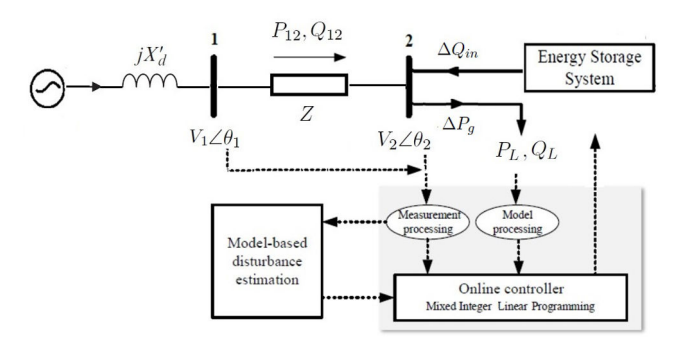


Fig. 3 Voltage control diagram with TLS satisfaction

(16)

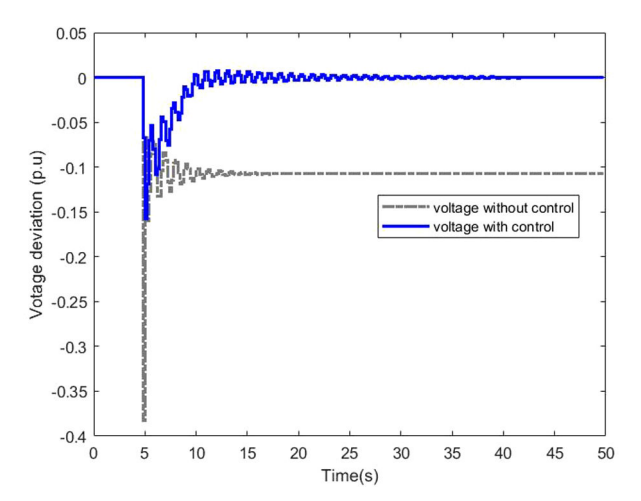


Fig. 4 Voltage deviation response without TLS

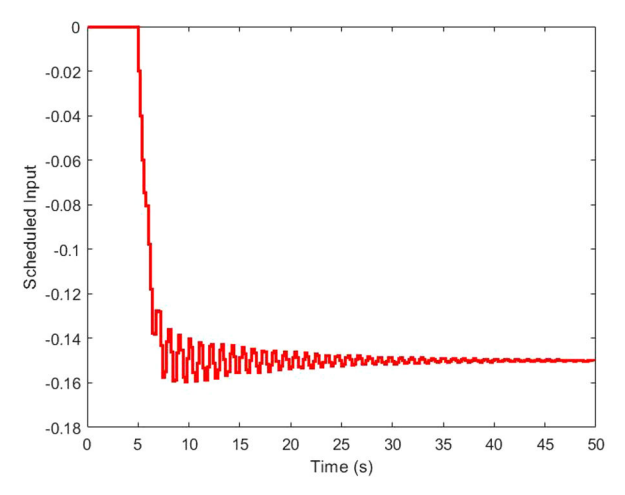


Fig. 5 Input signal for voltage control without TLS

The above TLS states that when the deviation of the voltage  $V_2$  following the perturbation is larger than  $\Delta V$ , it should become less than  $\Delta V$  within  $t_a$  seconds, for always. Since the ESS has limited capacity, the control input should be bounded and not exceeds a certain limit, i.e.  $|u(t_k)| \le U_{\text{lim}}$ .

Similar to the control synthesis in (3), let the scheduling horizon 0 < L < N and denote  $\mathcal{T} = [0, ..., H]$ , such that H = N - L is a finite horizon provided as a user input. The objective is to minimise the total control effort, which can be represented as the summation of all decision variables in the cost function given by

$$J(x_0, \mathbf{u}_k^L, \mathbf{w}_k^N) = \sum_{k=1}^H \left| u(t_k)^L \right|, \tag{24}$$

where the voltage is required to satisfy the TLS constraints described by  $\phi$  in (23),  $\forall k \in \mathcal{T}$ .

The scheduling problem can be summarised as follows:

$$u = \underset{u(t_k)^L}{\min} J(x_0, u_k^L, w_k^N),$$

$$s.t. \quad \forall k \in \mathcal{T}$$

$$X(t_{k+1}) = A_d X(t_k) + B_{d_1} u(t_k) + B_{d_2} \hat{d}(t_k)$$

$$\Delta V_2(t_{k+1}) = C_d X(t_k) + D_{d_1} u(t_k) + D_{d_2} \hat{d}(t_k)$$

$$|u(k)| \leq U_{\lim}, \quad \forall k \in \mathcal{T}$$

$$\Delta V_2(t_k) \models \phi, \quad \forall k \in \mathcal{H}$$

$$\phi = \Box [\neg (|\Delta V_2(k)| \leq \Delta V) \Rightarrow \diamondsuit_{[0,t_d]} \Box (|\Delta V_2(k)| \leq \Delta V)$$

The control u is the horizon-H control input computed at each time step  $t_k$ ,  $\forall k \in \mathcal{T}$ , such that u is computed as the first element of the sequence  $u_k^L = u(t_k)^L u(t_{k+1})^L, \dots, u(t_{k+L-1})^L$ .

In this study, the TLSs are encoded into a MILP using the toolbox BluSTL [26], and the overall problem is converted into a MILP and solved by the relevant solvers in Gurobi [27].

#### 3.4 Case studies

3.4.1 System parameters: Consider the linearised system (17). Note that all the following system parameters are in (p.u.) with values:

$$\omega_{\rm S} = 377 {
m rad/s}, \ H = 6 s, \ D = 0, \ T_{\rm A} = 0.05 {
m s}, \ T_{\rm g} = 0.2 {
m s}, \ T_{\tau} = 0.5 {
m s}, \ R = 0.05, \ T_{d_0} = 5 {
m s}, \ K = 50, \ X_d = 1.2, \ X'_d = 0.3, \ X_a = 1.1.$$

Equilibrium points of the algebraic variables

$$V_1 = 1.05 \text{ V}, \ V_2 = 0.983 \text{ V}, \ I_d = 0.6319 \text{ A}, \ I_q = 0.4489 \text{ A},$$
  
 $\theta_1 = 0^{\circ}, \ \theta_2 = -6.596^{\circ}.$ 

Operating points of the state variables are

$$\delta = 28.0522^{\circ}, \ E_q' = 1.1162, \ E_{\rm fd} = 1.5846, \ P_{\rm v} = 1.$$

The line impedance is given by

$$Z = 0.02 + j0.1728.$$

The load active and reactive power, in steady-state, are given by  $P_{\rm L}=0.716$  and  $Q_{\rm L}=0.26$ , respectively. The generator supplies electrical power  $S_{\rm G}=0.728+j0.3639$ . The perturbation is considered as a step-change in load demand and is given by  $\Delta P_{\rm g}=0.5$ .

3.4.2 MPC without TLSs: Before introducing the TLSs constraint, the MPC without TLSs is designed by considering that the objective is to minimise the control effort and the voltage deviation. Consider the state-space model (17) with the above parameters. The total control effort and the voltage deviation can be expressed by

$$\overline{J_U} = \sum_{k=1}^{T} \left[ \left| u(t_k)^L \right| + \left| \Delta V_2(t_k) \right| \right]. \tag{26}$$

Similar to (25), scheduling is summarised as follows:

$$\min \quad \overline{J_U}$$

$$s.t. \quad \forall k \in \mathcal{T}$$

$$X(t_{k+1}) = A_d X(t_k) + B_{d1} u(t_k) + B_{d2} \hat{d}(t_k)$$

$$\Delta V_2(t_{k+1}) = C_d X(t_k) + D_{d1} u(t_k) + D_{d2} \hat{d}(t_k)$$

$$|u(k)| \le U_{\lim}, \quad \forall k \in \mathcal{T}.$$

$$(27)$$

The simulation results in Fig. 4 represent the voltage deviation with control (without TLS) and without control, while Fig. 5 shows the control input. We remark that the voltage restoration takes more than 5s, and the problem is feasible for a control limit bound  $U_{\rm lim} = 0.2$ .

**3.4.3** MPC with TLSs: Consider now the state-space model (17) with the above parameters. Let the scheduling problem be

IET Energy Syst. Integr. 5

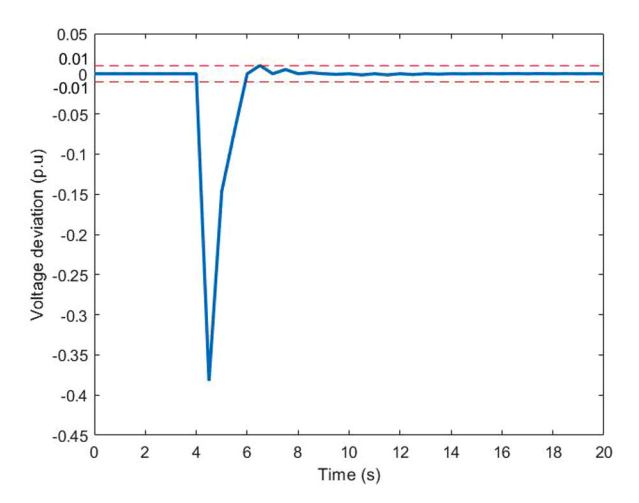


Fig. 6 Voltage deviation response for the "always" TLS scenario in (29)

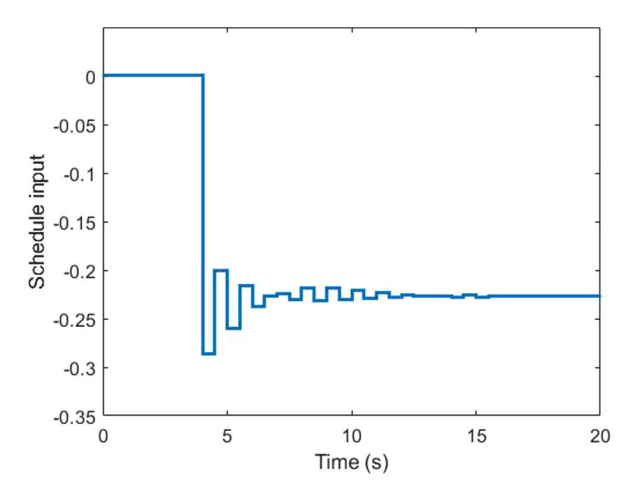


Fig. 7 Input signal for the "always" TLS scenario in (29)

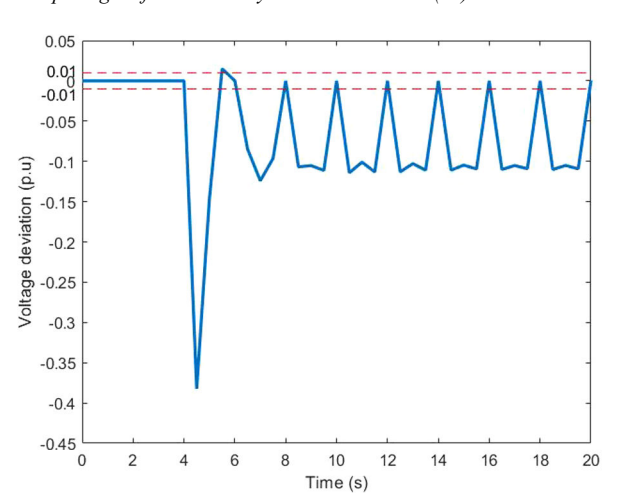


Fig. 8 Voltage deviation response for the "eventually" TLS scenario in (30)

$$\arg \min_{u(t_k)^L} J(x_0, u(t_k)^L, w) = \arg \min_{u(t_k)^L} \sum_{k=1}^H \left| u(t_k)^L \right|,$$

$$s.t. \quad \forall k \in \mathcal{T}$$

$$X(t_{k+1}) = A_d X(t_k) + B_{d1} u(t_k) + B_{d2} \hat{d}(t_k)$$

$$\Delta V_2(t_{k+1}) = C_d X(t_k) + D_{d1} u(t_k) + D_{d2} \hat{d}(t_k)$$

$$|u(k)| \le U_{\lim}, \quad \forall k \in \mathcal{T}$$

$$\Delta V_2(t_k) \models \phi, \quad \forall k \in \mathcal{T}$$

with  $U_{\text{lim}} = 0.4$ . We propose to constrain the voltage deviation to satisfy the following TLS for a finite-time voltage restoration:

$$\phi = \Box(\neg(|\Delta V_2| \le 0.01)) \Rightarrow (\Diamond_{[0,2]}\Box(|\Delta V_2| \le 0.01)), \tag{29}$$

which reads that 'when  $|\Delta V_2|$  is larger than 0.01, it should become less than 0.01 in less than 2s for always.' The simulation results for this TLS scenario are illustrated in Figs. 6 and 7. Note that the prediction horizon is given by H=4s. It can be observed in Fig. 6 that the voltage response satisfies the required TLS in (29).

Now, we want to design the input control for voltage restoration using the 'eventually' TLS scenario. Figs. 8 and 9 show the voltage deviation and the control input, respectively, according to the following TLS:

$$\phi = \Box(\neg(|\Delta V_2| \le 0.01)) \Rightarrow (\Diamond_{[0,2]}(|\Delta V_2| \le 0.01)). \tag{30}$$

The difference here from the TLS in (29) is that there is no specification of always (i.e.  $\Box$ ), that is, 'whenever  $|\Delta V_2|$  is larger than 0.01, it should become less than 0.01 in less than 2s eventually.' Results show that the controls with TLS in Figs. 6 and 8 were able to satisfy the required temporal specifications, while the control without TLS in Fig. 4 was unable to satisfy the specified temporal constraint. In summary, the proposed controller with TLSs guarantees to satisfy the temporal voltage specifications (finite-time restorations). While the control without TLSs may or may not satisfy the temporal voltage specifications; it is based on trial and error procedure.

#### 3.5 Generalisation to multi-machine systems

In this section, we generalise the proposed control approach to a multi-machine system by considering a microgrid consisting of an M-generator and N-load bus network. The dynamics of the overall system can be described by the following equations:

A. The linearised dynamic equations of each generator

$$\Delta \dot{\delta}_{i} = \omega_{si} \Delta \omega_{ri}$$

$$\Delta \dot{\omega}_{r} = \frac{1}{2H} [\Delta P_{mi} - I_{qi} \Delta E'_{qi} - (E'_{qi} + (X_{qi} - X'_{di})I_{di}) \Delta I_{qi}$$

$$-(X_{qi} - X'_{di})I_{qi} \Delta I_{di} - D_{i} \Delta \omega_{si}]$$

$$\Delta \dot{E}'_{qi} = \frac{-1}{T_{d_0}} [\Delta E'_{qi} + (X_{di} - X'_{di}) \Delta I_{di} - \Delta E_{fdi}]$$

$$\Delta \dot{E}_{fd} = \frac{-1}{T_{A}} [\Delta E_{fdi} - K_{i} (\Delta V_{refi} - \Delta V_{i})]$$

$$\Delta \dot{P}_{m} = \frac{-1}{T_{r}} [\Delta P_{mi} - P_{vi}]$$

$$\Delta \dot{P}_{v} = \frac{-1}{T_{g}} [\Delta P_{vi} - (\Delta P_{refi} - \frac{1}{R} \Delta \omega_{ri})]$$
(31)

Define the state of each generator as

$$X_i = [\delta_i \, \omega_{ri} \, E_{ai} \, E_{fdi} \, P_{mi} \, P_{vi}]^{\mathrm{T}}, \quad i = 1, ..., M$$
 (32)

Then the dynamical system (31) can be written as

$$\Delta \dot{X}_{i} = A_{1i} \Delta X_{i} + B_{1i} I_{gi} + B_{2i} \Delta V_{gi} + E_{1i} \Delta T_{i1}, \tag{33}$$

where

$$\Delta I_{gi} = \begin{bmatrix} \Delta I_{di} \\ \Delta I_{qi} \end{bmatrix}, \quad \Delta V_{gi} = \begin{bmatrix} \Delta V_i \\ \Delta \theta_i \end{bmatrix}, \quad \Delta T_{1i} = \begin{bmatrix} \Delta P_{\text{ref}i} \\ \Delta V_{\text{ref}i} \end{bmatrix}.$$
(34)

B. Stator equations of each generator

$$X_{qi}I_{qi} = V_i\sin(\delta_i - \theta_i),$$
  

$$E_{ai} - X'_{di} = V_i\cos(\delta_i - \theta_i).$$
(35)

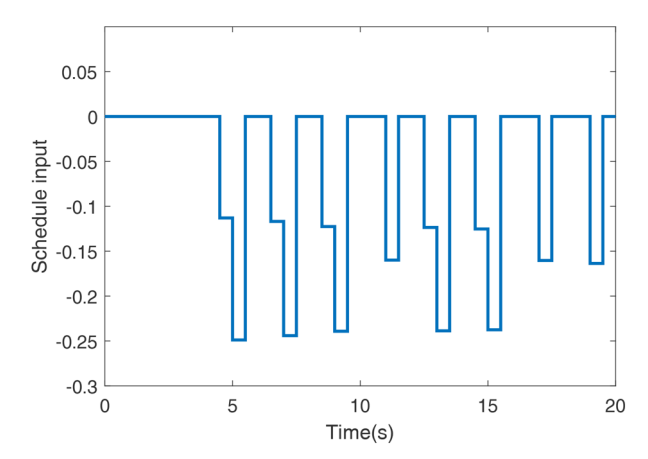


Fig. 9 Input signal for the "eventually" TLS scenario in (30)

By linearising the equations in (35), we get

$$\Delta I_{gi} = D_{1i} \Delta V_{gi} + D_{2i} \Delta X_i, \tag{36}$$

C. Network equations: The power flow equations for each generator bus are given by

$$I_{di}V_{i}\sin(\delta_{i} - \theta_{i}) + I_{qi}V_{i}\cos(\delta_{i} - \theta_{i}) + P_{Li}$$

$$= \sum_{k=1}^{m} V_{i}V_{k}Y_{ik}\cos(\theta_{i} - \theta_{k} - \alpha_{ik})$$

$$i = 1, ..., M,$$
(37)

$$I_{di}V_{i}\cos(\delta_{i} - \theta_{i}) - I_{qi}V_{i}\sin(\delta_{i} - \theta_{i}) + Q_{Li}$$

$$= \sum_{k=1}^{m} V_{i}V_{k}Y_{ik}\sin(\theta_{i} - \theta_{k} - \alpha_{ik})$$

$$i = 1, ..., M.$$
(38)

The power flow equations at the load buses are given by

$$\sum_{k=1}^{m} V_{i} V_{k} Y_{ik} (\theta_{i} - \theta_{k} - \alpha_{ik}) = P_{Li} - P_{di}$$

$$\sum_{k=1}^{m} V_{i} V_{k} Y_{ik} (\theta_{i} - \theta_{k} - \alpha_{ik}) = Q_{Li} + Q_{ui}$$

$$i = 1, ..., N.$$
(39)

where  $P_{di}$  is the perturbation (power change at bus i) and  $Q_{ui}$  is the control input from the ESS (the reactive power input).

From the linearisation of (37) and (38), we get

$$\Delta I_{gi} = C_{1i} \Delta V_{gi} + C_{2i} \Delta X_i + C_{3i} \Delta V_{li}. \tag{40}$$

where  $\Delta V_{li} = \begin{bmatrix} \Delta V_i \\ \Delta \theta_i \end{bmatrix}$  are the voltage and angle variations of the load buses, for i = 1, ..., N.

From the linearisation of (39), we get the expression of the voltage deviation as

$$\Delta V_{li} = \hat{C}_{1i} \Delta V_{gi} + \hat{C}_{2i} \Delta P_{di} + \hat{C}_{3i} \Delta Q_{ui}, \tag{41}$$

For an M-generator and N-load bus system, we can express (33), (36), (40) and (41) in a compact form as

$$\Delta \dot{X} = A_1 \Delta X + B_1 I_g + B_2 \Delta V_g + E_1 \Delta T_1$$

$$\Delta I_g = D_1 \Delta V_g + D_2 \Delta X$$

$$\Delta I_g = C_1 \Delta V_g + C_2 \Delta X + C_3 \Delta V_l$$

$$\Delta V_l = \hat{C}_1 \Delta V_g + \hat{C}_2 \Delta P_d + \hat{C}_3 \Delta Q_u,$$

$$(42)$$

where  $A_1$ ,  $B_1$ ,  $B_2$ ,  $T_1$  are block-diagonal matrices. By combining all the equations in (42), we get the following final state equation for the system:

$$\dot{X} = \hat{A}X + \hat{B}_u \Delta U_{\text{in}} + \hat{B}_w \Delta P_d 
\Delta V_I = \hat{C}X + \hat{D}_u \Delta U_{\text{in}} + \hat{D}_w \Delta P_d.$$
(43)

Now, the proposed control approach can be applied to this multimachine system in a similar way, as described in Section 3.3.

#### 4 Conclusion

In this paper, a new synthesising closed-loop controller for power grid systems subject to TLSs is presented. The controller formulation corresponds to an MPC scheme by introducing a time constraint. The power system model considered contains an SG connected to a critical load bus. To maintain the voltage within range and time constraints simultaneously following a perturbation, an ESS that is connected to the critical load bus supports the voltage restoration by injecting reactive power. The optimal reactive power input signal is computed from a MILP, where the TLSs are encoded, such that the voltage admits a restricted finite-time restoration. Future work will be devoted to multiple actuators scheduling using both active and reactive powers. Islanded microgrids with dynamic motor loads will be considered as well, where the delay in voltage recovery for an induction motor load under temporal constraints will be investigated.

## 5 Acknowledgment

This manuscript was authored by UT-Battelle, LLC, under Contract No. DE-AC05-00OR22725 with the U.S. Department of Energy. The United States Government retains and the publisher, by accepting the article for publication, acknowledges that the United States Government retains a non-exclusive, paid-up, irrevocable, worldwide license to publish or reproduce the published form of this manuscript, or allow others to do so, for United States Government purposes. The Department of Energy will provide public access to these results of federally sponsored research in accordance with the DOE Public Access Plan (http://energy.gov/ downloads/doe-public-access-plan). Research sponsored by the Laboratory Directed Research and Development Program of Oak Ridge National Laboratory (ORNL), managed by UT-Battelle, LLC for the U.S. Department of Energy under Contract No. DE-AC05-00OR22725. In addition, this research sponsored in part by the Engineering Research Center Program of the National Science Foundation and the Department of Energy under NSF Award Number EEC-1041877 and the CURRENT Industry Partnership Program. The third author was supported in part by the National Science Foundation under NSF-ECCS-Awards 1711432 and 1509114 and by a Joint Directed Research and Development (JDRD) grant.

## 6 References

- Kundur, P.: 'Power system stability and control' (McGraw-Hill New York, New York, NY, 1994)
- [2] Mohod, S. W., Aware, M.V.: 'Micro wind power generator with battery energy storage for critical load', *IEEE Syst. J.*, 2012, 6, (1), pp. 118–125
   [3] Delfino, F., Pampararo, R., Rossi, M.: 'A feedback linearization control
- [3] Delfino, F., Pampararo, R., Rossi, M.: 'A feedback linearization control scheme for the integration of wind energy conversion systems into distribution grids', *IEEE Syst. J.*, 2012, 6, (1), pp. 85–93
   [4] Xu, Z., Julius, A., Chow, J.H.: 'Robust testing of cascading failure mitigations
- [4] Xu, Z., Julius, A., Chow, J.H.: 'Robust testing of cascading failure mitigations based on power dispatch and quick-start storage', *IEEE Syst. J.*, 2018, 12, (4), pp. 3063–3074
   [5] Srivastava, A.K., Kumar, A.A., Schulz, N.N.: 'Impact of distributed
- [5] Srivastava, A.K., Kumar, A.A., Schulz, N.N.: 'Impact of distributed generations with energy storage devices on the electric grid', *IEEE Syst. J.*, 2012, 6, (1), pp. 110–117
- [6] Deng, Z., Xu, Y., Sun, H., et al.: 'Distributed, bounded and finite-time convergence secondary frequency control in an autonomous microgrid', IEEE Trans. Smart Grid, 2019, 10, (3), pp. 2776–2788
- [7] Zhang, Y., Tomsovic, K., Djouadi, S., et al.: 'Hybrid controller for wind turbine generators to ensure adequate frequency response in power networks', *IEEE J. Emerg. Sel. Top. Circuits Syst.*, 2017, 7, (3), pp. 359–370
- [8] Zhang, Y., Raoufat, M.E., Tomsovic, K., et al.: 'Set theory based safety supervisory control for wind turbines to ensure adequate frequency response', *IEEE Trans. Power Syst.*, 2019, 34, (1), pp. 680–692

- [9] Zuo, S., Davoudi, A., Song, Y., et al.: 'Distributed finite-time voltage and frequency restoration in islanded AC microgrids', IEEE Trans. Ind. Electron., 2016 63 (10) pp. 5988–5997
- 2016, 63, (10), pp. 5988–5997
   Guo, F., Wen, C., Mao, J., et al.: 'Distributed secondary voltage and frequency restoration control of droop-controlled inverter-based microgrids', IEEE Trans. Ind. Electron., 2015, 62, (7), pp. 4355–4364
- [11] Lou, G., Gu, W., Xu, Y., et al.: 'Distributed MPC-based secondary voltage control scheme for autonomous droop-controlled microgrids', *IEEE Trans.* Sustain. Energy, 2017, 8, (2), pp. 792–804
- Sustain. Energy, 2017, 8, (2), pp. 792–804

  [12] Simpson-Porco, J.W., Shafiee, Q., Dörfler, F., et al.: 'Secondary frequency and voltage control of islanded microgrids via distributed averaging', IEEE Trans. Ind. Electron., 2015, 62, (11), pp. 7025–7038
- [13] Bidram, A., Davoudi, A., Lewis, F.L., et al.: 'Secondary control of microgrids based on distributed cooperative control of multi-agent systems', *IET Gener. Transm. Distrib.*, 2013, 7, (8), pp. 822–831
- [14] Bidram, A., Davoudi, A., Lewis, F.L., et al.: 'Distributed cooperative secondary control of microgrids using feedback linearization', IEEE Trans. Power Syst., 2013, 28, (3), pp. 3462–3470
- [15] Xu, Z., Julius, A., Chow, J.H.: 'Energy storage controller synthesis for power systems with temporal logic specifications', *IEEE Syst. J.*, 2019, 13, (1), pp. 748–759
- [16] Xu, Z., Julius, A., Chow, J.H.: 'Coordinated control of wind turbine generator and energy storage system for frequency regulation under temporal logic specifications'. Proc. of the American Control Conf. (ACC), Milwaukee, WI, USA, 2018, pp. 1580–1585
- [17] Zhang, Y., Olama, M., Melin, A., et al.: 'Synthesizing distributed energy resources in microgrids with temporal logic specifications'. Proc. of the IEEE Int. Symp. Power Electron. Distrib. Gener. Syst. (PEDG), Charlotte, NC, USA, 2018, pp. 1–7
- [18] Zhang, Y., Taousser, F., Olamay, M., et al.: 'Secondary voltage control via demand-side energy storage with temporal logic specifications'. Proc. of the 10th Conf. on Innovative Smart Grid Technologies (ISGT), Washington, DC, USA, 2019, pp. 1–5
- [19] Xu, Z., Federico, Z., Wu M, B., et al.: 'Controller synthesis for multi-agent systems with intermittent communication: A metric temporal logic approach'. Proc. of the 57th Annual Allerton Conf. on Communication, Control and Computing, Monticello, IL, USA, 2019, pp. 1015–1022
- [20] Kress-Gazit, H., Fainekos, G., Pappas, G.: 'Temporal-logic-based reactive mission and motion planning', *IEEE Trans. Robot.*, 2009, 25, (6), pp. 1370–1381
- [21] Wongpiromsarn, T., Topcu, U., Murray, M.R.: 'Receding horizon temporal logic planning', *IEEE Trans. Autom. Control*, 2012, 57, (11), pp. 2817–2830
- [22] Raman, V., Donze, A., Maasoumy, M., et al.: 'Model predictive control with signal temporal logic specifications'. Proc. of the 53rd IEEE Conf. on Decision and Control (CDC), Los Angeles, CA, USA, 2014, pp. 81–87
- [23] Gevorgian, V., Bezrukikh, P., Karghiev, V.: 'Wind-diesel hybrid systems for Russia's northern territories', Nat. Renew. Energy Lab., Golden, CO., USA, Tech. Rep. NREL/CP-500-27114, 1999
- [24] Allen, R., Brutkoski, D., Farnsworth, D., et al.: 'Sustainable energy solutions for rural Alaska', Lawrence Berkeley Nat. Lab., Berkeley, CA, USA, Tech. Rep. LBNL-1005097, 2016
- [25] Wongpiromsarn, T., Topcu, U., Murray, M.R.: 'An MILP approach for real-time optimal controller synthesis with metric temporal logic specifications'. Proc. of the American Control Conf. (ACC), Boston, MA, USA, 2016, pp. 1105–1110
- [26] Donzé, A., Raman, V., Frehse, G., et al.: 'Blustl: controller synthesis from signal temporal logic specifications'. Proc. of the 1st and 2nd Int. Workshop on Applied Verification for Continuous and Hybrid Systems, Seattle, WA, USA, 2015, pp. 160–168
- [27] Gurobi Optimizer, Gurobi ApS, [Online]. Available at http://www.gurobi.com/documentation/8.0/quickstartwindows.pdf, 2018

## 7 Appendix

Denote by  $\theta_1^0, \theta_2^0, \delta^0, V_1^0$ , and  $V_2^0$  the steady-state parameters of  $\theta_1, \theta_2, \delta, V_1$ , and  $V_2$ , respectively. Define

$$\delta^{0} - \theta_{2}^{0} = \gamma_{0}, \ \Lambda = \ \det \begin{bmatrix} -R_{\mathrm{e}} & (X_{q} + X_{\mathrm{e}}) \\ -(X_{\mathrm{e}} + X'_{d}) & -R_{\mathrm{e}} \end{bmatrix}$$

The constants used in this paper are given as follows:

$$\alpha_{1} = \left(\frac{1}{\Lambda}\right) \left[ -R_{e} \sin(\gamma_{0}) - (X_{q} + X_{e}) \cos(\gamma_{0}) \right]$$

$$\alpha_{2} = \left(\frac{V_{2}^{0}}{\Lambda}\right) \left[ -R_{e} \cos(\gamma_{0}) + (X_{q} + X_{e}) \sin(\gamma_{0}) \right]$$

$$\alpha_{3} = \left(\frac{1}{\Lambda}\right) \left[ (X'_{d} + X_{e}) \sin(\gamma_{0}) - R_{e} \cos(\gamma_{0}) \right]$$

$$\alpha_{4} = \left(\frac{V_{2}^{0}}{\Lambda}\right) \left[ R_{e} \sin(\gamma_{0}) + (X'_{d} + X_{e}) \cos(\gamma_{0}) \right]$$

$$\alpha_{5} = \left(\frac{1}{\Lambda}\right) \left[ X_{q} + X_{e} \right], \quad \alpha_{6} = \left(\frac{R_{e}}{\Lambda}\right)$$

$$\alpha_{7} = \left(\frac{-\cos(\delta^{0} - \theta_{1}^{0})}{X'_{d}}\right), \quad \alpha_{8} = \left(\frac{V_{1} \sin(\delta^{0} - \theta_{1}^{0})}{X'_{d}}\right), \quad \alpha_{9} = \left(\frac{1}{X'_{d}}\right)$$

$$\alpha_{10} = \left(\frac{\sin(\delta^{0} - \theta_{1}^{0})}{X_{q}}\right), \quad \alpha_{11} = \left(\frac{V_{1} \cos(\delta^{0} - \theta_{1}^{0})}{X_{q}}\right).$$
Let  $\Lambda' = \det \begin{bmatrix} \alpha_{7} & \alpha_{8} \\ \alpha_{10} & \alpha_{11} \end{bmatrix}, \text{ we have}$ 

$$\beta_{1} = \left(\frac{1}{\Lambda'}\right) \left[\alpha_{11}\alpha_{1} - \alpha_{8}\alpha_{3}\right], \quad \beta_{2} = \left(\frac{1}{\Lambda'}\right) \left[\alpha_{11}\alpha_{2} - \alpha_{8}\alpha_{4}\right]$$

$$\beta_{3} = \left(\frac{1}{\Lambda'}\right) \left[\alpha_{10}\alpha_{1} - \alpha_{7}\alpha_{3}\right], \quad \beta_{4} = \left(\frac{1}{\Lambda'}\right) \left[\alpha_{10}\alpha_{2} - \alpha_{7}\alpha_{4}\right]$$

$$\beta_{5} = \left(\frac{1}{\Lambda'}\right) \left[\alpha_{11}(\alpha_{5} - \alpha_{9}) - \alpha_{8}\alpha_{6}\right]$$

$$\beta_{6} = \left(\frac{1}{\Lambda'}\right) \left[\alpha_{10}(\alpha_{5} - \alpha_{9}) - \alpha_{7}\alpha_{6}\right]$$

Introducing the above identities in the linearised equations of the SG, we get

$$\begin{split} K_1 &= E_q \alpha_4 + (X_q - X'_d)(I_d \alpha_4 + I_q \alpha_2) \\ K_2 &= I_q + E_q \alpha_6 + (X_q - X'_d)(I_d \alpha_6 + I_q \alpha_5) \\ K_3 &= E_q \alpha_3 + (X_q - X'_d)(I_d \alpha_3 + I_q \alpha_1) \\ K_4 &= (X_d - X'_d)\alpha_2, \ K_5 = 1 + \alpha_5(X_d - X'_d) \\ K_6 &= (X_d - X'_d)\alpha_1 \end{split}$$

Let  $\theta_{21}^0 = \theta_2^0 - \theta_1^0$ . From the linearisation of the power flow equations, we have

$$\begin{split} c_1 &= 2V_2G_{12} - V_1[G_{21}\mathrm{cos}(\theta_{21}^0) - B_{21}\mathrm{sin}(\theta_{21}^0)] \\ c_2 &= -V_2[G_{21}\mathrm{cos}(\theta_{21}^0) - B_{21}\mathrm{sin}(\theta_{21}^0)] \\ c_3 &= V_1V_2[ - G_{21}\mathrm{sin}(\theta_{21}^0) - B_{21}\mathrm{cos}(\theta_{21}^0)] \\ c_4 &= 2V_2B_{21} - V_1[G_{21}\mathrm{sin}(\theta_{21}^0) + B_{21}\mathrm{cos}(\theta_{21}^0)] \\ c_5 &= -V_2[G_{21}\mathrm{sin}(\theta_{21}^0) + B_{21}\mathrm{cos}(\theta_{21}^0)] \\ c_6 &= V_1V_2[G_{21}\mathrm{cos}(\theta_{21}^0) - B_{21}\mathrm{sin}(\theta_{21}^0)] \,. \end{split}$$

Let  $\gamma = (c_3c_4 - c_1c_6) + \beta_1(c_3c_5 - c_6c_2)$ . And the constants  $\gamma_1 - \gamma_4$  are given by

$$\gamma_1 = \frac{-\beta_2}{\gamma} (c_3 c_5 - c_6 c_2), \ \gamma_2 = \frac{-\beta_5}{\gamma} (c_3 c_5 - c_6 c_2),$$
$$\gamma_3 = \frac{c_3}{\gamma}, \ \gamma_4 = \frac{c_6}{\gamma}.$$

The constants  $K'_1 - K'_{12}$  of the linearised system (18) are given by

$$K'_{1} = K_{1} + K_{3}\gamma_{1}, K'_{2} = K_{2} + K_{3}\gamma_{2}, K'_{3} = K_{3}\gamma_{3}$$
  
 $K'_{4} = K_{3}\gamma_{4}, K'_{5} = K_{4} + K_{6}\gamma_{1}, K'_{6} = K_{5} + K_{6}\gamma_{2}$   
 $K'_{7} = K_{6}\gamma_{3}, K'_{8} = K_{6}\gamma_{4}, K'_{9} = \beta_{1}\gamma_{1} + \beta_{2}$   
 $K'_{10} = \beta_{1}\gamma_{2} + \beta_{5}, K'_{11} = \beta_{1}\gamma_{3}, K'_{12} = \beta_{1}\gamma_{4}$